Retrieval of source parameters for local earthquakes in anisotropic media

D. Rößler[1], I. Pšenčík[2], F. Krüger[1], G. Rümpker[3]

[1]Department of Geosciences, University of Potsdam, Postfach 601553, 14415 Potsdam, FR Germany. E-mail: diroess@rz.uni-potsdam.de
[2]Geophysical Institute, Academy of Sciences of the Czech Republic, Bocni II/1401, 14131 Prague 4, Czech Republic,
[3]Department of Meteorology and Geophysics, University of Frankfurt/Main, Feldbergstr. 47, 60323 Frankfurt am Main, FR Germany

1 Summary

An inversion scheme to retrieve the characteristic of seismic point sources in anisotropic media is proposed.

Moment tensors retrieved from waves generated by point sources in anisotropic media may be biased if isotropy is assumed during inversion. Apparent volumetric components may be obtained for shear sources and falsely interpreted in terms of tensile earthquakes. Similarly, real volumetric components due to tensile faulting may not be visible in retrieved moment tensors.

Instead of the moment tensor the geometry of the source is retrieved directly in our inversion. The source geometry is defined by the orientation of the slip vector and the fault normal as well as the strength of the event given by the length of the slip and the area of the fault. The source geometry may be used to calculate the moment tensor. Our tests show that approximating structural inhomogeneity instead of using homogeneous models is important to retrieve the orientation of the source. However, accounting for inhomogeneity and anisotropy during inversion yields more complete solutions. This allows accurate interpretation of the source geometry in terms of shear and tensile faulting to identify volumetric source changes that occur during rupturing.

2 Introduction

Seismic moment tensors describe the orientation and the strength of point sources. To obtain information about volumetric changes at the seismic source that occur during rupturing (tensile earthquakes) the moment tensor may be decomposed into the double-couple component that quantifies the amount of shear faulting, the compensated-linear-vector-dipole and the isotropic component that provides information on the volumetric source changes (*Jost* and *Herrmann*, 1989; *Aki* and *Richards*, 2002). Moment tensors are routinely determined under the assumption that the medium at the source and along the ray-path is isotropic. That means that anisotropic material properties are usually neglected during inversion. However, due to anisotropy the radiation pattern of seismic sources may be distorted and moment tensors may comprise apparent volumetric components or true volumetric components may not be visible (see e.g. *Kawasaki* and *Tanimoto*, 1981; *Ben-Menahem et al.*, 1991; *Gajewski*, 1993; *Julian et al.*, 1998; *Rößler et al.*, 2004, 2005; *Vavryčuk*, 2005). The effect of anisotropy on moment tensors is also dependend on the orientation of the anisotropic elastic tensor with respect to the source.

In practice, volumetric source components are frequently observed (see e.g. *Sykes*, 1967; *Solomon* and *Julian*, 1974; *Julian et al.*, 1997; *Horálek et al.*, 2000; *Dahm et al.*, 2000; *Vavryčuk*, 2002; *Foulger et al.*, 2004; *Vavryčuk*, 2002). Observed volumetric components may be indicative of the role of fluids during rupturing and mineral phase changes at greater depth or may image existing pathways enabling fluid migration in carbonhydrate production fields. In these cases their accurate determination is of primary interest. Without knowledge of the anisotropic elastic constants at the source, the reliability of interpretations of the moment tensor in terms of volumetric source changes must be questioned (*Rößler et al.*, 2005; *Vavryčuk*, 2005). We therefore propose an inversion scheme to directly invert observed seismograms for the direction of slip and fault normal for sources in inhomogeneous and anisotropic media. Efficiency and stability of the inversion scheme is demonstrated by means of inversion of synthetic seismograms for anisotropic media. Hereby we assume an event and station configuration that was typical in the swarm earthquake area W-Bohemia/Vogtland in Central Europe in the year 2000. During that time several institutions operated permanent and temporary networks to monitor the seismicity in this area. Furthermore, the structure of this area has been intensively studied in recent time and different velocity model are available now. In our testing we use the models proposed by *Vavryčuk* (1993) and *Málek et al.* (2005) (see Fig. 1). The first model is homogeneous and anisoptropic. It has been derived from travel time differences of qP and qS waves. The second model is inhomogeneous and weakly anisotropic. It has been determined from travel times of qP waves only. An important feature of this model is a strong near-surface velocity gradient. The elastic parameters are given in the representation of the weak anisotropy parameters (*Farra* and *Pšenčík*, 2003). Also an isotropic reference model is given therein. However, this model contains no information on the elastic moduli that are only determined by the shear waves. We therefore compile the two anisotropic models of *Vavryčuk* (1993) and *Málek et al.* (2005) to one model by fixing the P-wave velocities determined by the inhomogeneous model (herein, the resulting model will be called the compiled model).

3 Scheme of inversion

For seismic waves travelling in inhomogeneous anisotropic media the i-th component of the displacement u_i in the far-field at $\mathbf{x}$ due to a point source at $\mathbf{x}_0$ is given in the ray-theoretical high-frequency approximation (*Pšenčík* and *Teles*, 1996) by:

$$u_i(\mathbf{x},t) = g_i(\mathbf{x}) \left[\frac{\rho(\mathbf{x}_0)c(\mathbf{x}_0)}{\rho(\mathbf{x})c(\mathbf{x})}\right]^{1/2} \frac{D f^{(A)}(t-\tau(\mathbf{x}))}{|\Omega_M(\mathbf{x})|^{1/2}} \exp\left[i\frac{\pi}{2}k_s - i\frac{\pi}{2}k(\mathbf{x}_0,\mathbf{x})\right], \tag{1}$$

where D denotes the directivity given by

$$D(\mathbf{x}_0,\theta,\phi) = \frac{g_j(\mathbf{x}_0) M_{jk}\, p_k(\mathbf{x}_0)}{4\pi\rho(\mathbf{x}_0)c(\mathbf{x}_0)}. \tag{2}$$

The directivity (2) depends on the moment tensor M_{jk} and the vector of polarisation g_j as well as on the slowness vector p_k, the phase velocity c and the density ρ at the source.

In (1), Ω_m is related to the relative geometrical spreading, $g_i(\mathbf{x})$ is the polarisation vector at x_m, and $f^{(A)}$ is the analytical signal corresponding to the source time function. The integer quantities k and k_s are related to the principal curvatures of the slowness surface at the receiver and at the source for the particular wave type (see *Pšenčík* and *Teles*, 1996, for a detailed description).

The moment tensor M_{jk} is given by the source geometry described by the direction of the slip s_p, the normal to the fault plane n_q (both vectors have unit length) as well as the elastic moduli c_{jkpq} that describe the medium in the vicinity of the source and a scalar quantity S formed by the product of the fault area and the length of the slip:

$$M_{jk} = s_p n_q c_{pqjk} S. \tag{3}$$

From (3) we see that, beside the source geometry, the moment tensor is influenced by the elastic properties at the source. Therefore, different properties of the moment tensor will arise from sources in isotropic and anisotropic media. As an example, shear faulting in anisotropic media may produce moment tensors with the character of tensile earthquakes, i.e. shear faulting accompanied by some amount of opening or closing of the fault during rupturing (see e.g. *Rößler et al.*, 2004; *Vavryčuk*, 2005).

Inserting (2) and (3) into (1) we can express the observed displacements in terms of 6 elementary sources σ_i representing elements of the source vector

$$\sigma_i = S(s_1 n_1, s_1 n_2 + s_2 n_1, s_1 n_3 + s_3 n_1, s_2 n_2, s_2 n_3 + s_3 n_2, s_3 n_3)^T, \tag{4}$$

$$u_i(\mathbf{x}, t) = A_i \frac{g_j(\mathbf{x_0}) p_k(\mathbf{x_0}) M_{jk}}{(4\pi\rho(\mathbf{x_0})c(\mathbf{x_0}))^{1/2}} f(t - \tau(\mathbf{x})) \exp\left[i\frac{\pi}{2}k_s - i\frac{\pi}{2}k(\mathbf{x_0}, \mathbf{x})\right] \tag{5}$$

$$= A_i B_{jk} s_p n_q c_{pqjk} S f(t - \tau(\mathbf{x})) \exp\left[i\frac{\pi}{2}k_s - i\frac{\pi}{2}k(\mathbf{x_0}, \mathbf{x})\right], \tag{6}$$

$$= Y_{il}\sigma_l f(t - \tau(\mathbf{x})) \exp\left[i\frac{\pi}{2}k_s - i\frac{\pi}{2}k(\mathbf{x_0}, \mathbf{x})\right]. \tag{7}$$

In (5) to (7) we use the following notations:

$$A_i = \frac{g_i(\mathbf{x})}{(\rho(\mathbf{x})c(\mathbf{x}))^{1/2}} \frac{1}{\Omega_M(\mathbf{x})} \tag{8}$$

$$B_{jk} = \frac{g_j(\mathbf{x_0}) p_k(\mathbf{x_0})}{(4\pi\rho(\mathbf{x_0})c(\mathbf{x_0}))^{1/2}} \tag{9}$$

$$\begin{aligned}
X_{i1} &= A_i B_{11}, \\
X_{i2} &= A_i (B_{12} + B_{21}), \\
X_{i3} &= A_i (B_{13} + B_{31}), \\
X_{i4} &= A_i B_{22}, \\
X_{i5} &= A_i (B_{23} + B_{32}), \\
X_{i6} &= A_i B_{33}, \\
Y_{i1} &= X_{i1}c_{1111} + X_{i2}c_{1112} + X_{i3}c_{1113} + X_{i4}c_{1122} + X_{i5}c_{1123} + X_{i6}c_{1133} \\
Y_{i2} &= X_{i1}c_{1211} + X_{i2}c_{1212} + X_{i3}c_{1213} + X_{i4}c_{1222} + X_{i5}c_{1223} + X_{i6}c_{1233} \\
Y_{i3} &= X_{i1}c_{1311} + X_{i2}c_{1312} + X_{i3}c_{1313} + X_{i4}c_{1322} + X_{i5}c_{1323} + X_{i6}c_{1333} \\
Y_{i4} &= X_{i1}c_{2211} + X_{i2}c_{2212} + X_{i3}c_{2213} + X_{i4}c_{2222} + X_{i5}c_{2223} + X_{i6}c_{2233} \\
Y_{i5} &= X_{i1}c_{2311} + X_{i2}c_{2312} + X_{i3}c_{2313} + X_{i4}c_{2322} + X_{i5}c_{2323} + X_{i6}c_{2333} \\
Y_{i6} &= X_{i1}c_{3311} + X_{i2}c_{3312} + X_{i3}c_{3313} + X_{i4}c_{3322} + X_{i5}c_{3323} + X_{i6}c_{3333}.
\end{aligned} \tag{10}$$

Eq. (7) relates the quantities Y_{ij} corresponding to the elementary sources σ_i to the observed seismograms. Thus, Y_{ij} will be called the elementary seismograms. We are therefore able to derive the source geometry from observed seismograms without referring to the moment tensor.

From σ_i we can calculate the slip inclination δ, i.e. the angle between the direction of the slip and the fault normal:

$$\delta = cos^{-1}\left(\sqrt{\frac{\sigma_1^2+\sigma_4^2+\sigma_6^2}{\sigma_i\sigma_i - 2\left(\sigma_1\sigma_4+\sigma_1\sigma_6+\sigma_4\sigma_6\right)}}\right), \quad for\ \sigma_1+\sigma_4+\sigma_6 \geq 0,$$

$$\delta = \pi - cos^{-1}\left(\sqrt{\frac{\sigma_1^2+\sigma_4^2+\sigma_6^2}{\sigma_i\sigma_i - 2\left(\sigma_1\sigma_4+\sigma_1\sigma_6+\sigma_4\sigma_6\right)}}\right), \quad for\ \sigma_1+\sigma_4+\sigma_6 < 0.$$

For pure shear faulting $\delta = 90°$. In the case of tensile earthquakes volumetric source changes occur and $\delta \gtrless 90°$.

The moment tensor, which is usually sought in seismological practice, may be immediately computed from (3) and (4):

$$M_{ij} = \sigma_1 c_{11ij} + \sigma_2 c_{12ij} + \sigma_3 c_{13ij} + \sigma_4 c_{22ij} + \sigma_5 c_{23ij} + \sigma_6 c_{33ij}. \tag{11}$$

In order to compare the retrieved source geometry with the (real or apparent) characteristics of the moment tensor we may decompose the moment tensor into its double-couple (DC), compensated-linear-vector-dipole (CLVD) and isotropic (ISO) components. The DC and CLVD components are frequently called the deviatoric components and the ISO is referred to as the volumetric component. The ISO describes (real or apparent) volumetric source changes connected to the faulting process. Real volumetric source changes will be also expressed in the slip inclination δ. Several different decompositions have been proposed (see e.g. *Silver* and *Jordan*, 1982; *Jost* and *Herrmann*, 1989; *Vavryčuk*, 2002). Herein we use the method of *Vavryčuk* (2002).

As a measure of strength of the event we calculate the moment magnitude $\mathrm{M_w}$ from the moment tensor (*Silver* and *Jordan*, 1982; *Bormann*, 2002):

$$\mathrm{M_w} = 2./3. * (log_{10}(\mathrm{M_0}) - 9.1), \tag{12}$$

$$\text{where } \mathrm{M_0} = \sqrt{\Sigma_{ij} M_{ij}^2/2}. \tag{13}$$

We seek the source vector σ_i by inversion of seismograms $u_j(x_k, t)$ observed from body waves that have propagated in anisotropic media. The inversion is carried out in the time domain. We use a least square approach to minimise the squared misfit between observations and predicted seismograms given by the left and the right handside of Eq. (7), respectively (*Menke*, 1989). The elementary seismograms Y_{ij} are computed for inhomogeneous anisotropic media using the software package ANRAY provided by the consortium project SW3D. By means of ANRAY waveforms of body waves in inhomogeneous, anisotropic media may be calculated using the ray-theoretical high-frequency approximation given in *Pšenčík* and *Teles* (1996).

Misalignment of data and elementary seismograms often occurs due to inaccurate phase picking. For time-domain inversion this may cause spurious non-shear components in retrieved source geometries. Phase alignment is therefore carried out in 3 steps prior to inversion.

1) Observed phases are manually picked. A time window for inversion is defined.

2) Within the time window the phases are manually aligned with the computed elementary seismograms.

3) Automatic cross-correlation is applied as part of the inversion code. A threshold based upon the correlation coefficient may be used to define if data are included in inversion.

4 Stability test

Incomplete knowledge of the earth's structure is expressed in simplified or inaccurate velocity and density models causing mismodelling of waveforms and errors earthquake localisation. Therefore, we test the sensitivity of the inversion scheme to mismodelling of the velocity structure and the hypocentre depth. To that aim, we invert synthetic waveforms assuming different (exact and inexact) velocity models for the calculation of the elementary seismograms Y_{ij} in (7).

We calculate synthetic waveforms of direct qP waves for one event in the compiled model (vertically inhomogeneous anisotropic model compiled from models by (*Vavryčuk*, 1993) and (*Málek et al.*, 2005) and invert them for the source geometry (see Fig. 3 for vertical-component seismograms). The velocity model is weakly anisotropic for P and S waves. The synthetic event is located at 9 km depth. Similar to many observations in W-Bohemia/Vogtland (*Dahm et al.*, 2000; *Horálek et al.*, 2000; *Wirth et al.*, 2000) this event has left-lateral vertical strike-slip focal mechanism ($n_i = (0, 1, 0)$, $s_i = 1, 0, 0$, $\sigma_i = (0, 1, 0, 0, 0, 0)$) and $M_w = 1.0$. Due to near-source anisotropy this pure shear source produces apparent non-double-couple components: DC=93.6%, CLVD=5.166%, ISO=1.3%. We further use a station-event distribution typical for the year 2000 earthquake swarm in W-Bohemia/Vogtland (see Fig. 2).

To test the sensitivity of the inversion to mismodelled velocity structure we invert synthetic P-wave seismograms for the source vector assuming three different velocity models for computation of elementary seismograms (for model representation see Fig. 1).
Model I: the correct medium (compiled vertically inhomogeneous anisotropic medium,
Model II: the isotropic approximation of the correct medium (vertically inhomogeneous isotropic medium, *Málek et al.*, 2005),
Model III: the homogeneous anisotropic medium (*Vavryčuk*, 1993).
During inversion the source depth is kept fixed at the correct position (9 km depth). Since anisotropy is weak in Model I ray paths and take-off angles at the source are virtually equal in Model I and II. Larger differences occur compared with rays in homogeneous Model III. Here, rays are straight. The main differences can be found for stations at larger distances where ray bending is stronger than at close distances due to the effect of the velocity gradient in the near-surface layer.

As expected the source vector can be retrieved with high precision if velocity model and source depth are known correctly during inversion (Model I, see Tab. 1 and Figs. 7, 6A for source properties and fit of waveforms). Corresponding moment tensor components as well as M_w equal the properties of the true source in Model I. The remaining residual and the variances of the source vector components are small indicating a high confidence level of the retrieved source. On the other hand the cross-correlation coefficients may reach large values for some elements σ_i (see Fig. 6B) showing strong coupling. However, since all elements of σ_i except of σ_2 are small ($\sigma_i/\sigma_2 \ll 1 \; \forall \; i \neq 2$) the strong correlations do not significantly influence the retrieved source geometry.

Introducing model inaccuracy during inversion we may expect erroneously retrieved source components. The Models I and II are similar as are resulting ray paths (see Figs.: 4 and 5). Using Model II instead of the true Model I for computation of Y_{ij} the retrieved components of the source vector and M_w agree well with the true source model (see Tab. 1 and Fig. 6A). Again, inaccuracies are small but strong correlation occurs between some elements (Fig. 6B). We are able to fit the waveforms at most stations (relative residual=0.02, see Fig. 8).

In contrast to the true source geometry, the retrieved source shows a small amount of

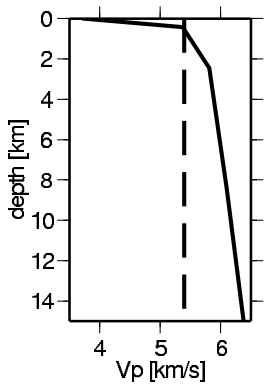

Figure 1: Isotropic reference P-wave velocity models for W-Bohemia/Vogtland. Solid line: vertically inhomogeneous model derived by *Málek et al.* (2005); dashed line: homogeneous model averaged from the homogeneous anisotropic model of *Vavryčuk* (1993) ($v_p = \sqrt{(C_{11} + C_{22} + C_{33})/3}$).

Table 1: Source vector components retrieved from synthetic seismograms using different velocity models and data residuals. Source vector used for computation of synthetic seismograms: $\sigma_i = (0, 1, 0, 0, 0, 0)$.

model	residual	σ_1	σ_2	σ_3	σ_4	σ_5	σ_6
I	0.00	-0.26E-04	0.10E+01	-0.10E-04	0.73E-04	-0.60E-04	-0.22E-04
II	0.02	0.46E-02	0.97E+00	0.78E-02	0.17E-01	-0.19E-01	-0.12E-01
III	0.03	0.68E-02	0.70E+00	0.14E-01	0.32E-01	-0.39E-01	-0.11E-01

faulting-related volumetric changes: $\delta = 89.4°$. The moment tensor calculated for this source comprises non-double components which are slightly different from the true source using Model I: DC=91.6%, CLVD=5.9%, ISO=2.6%.

The Model III is homogeneous and anisotropic. Rays propagating in this medium are straight. We may therefore expect effects on source retrieval by differences in ray path, take-off and incidence angles compared to rays in the models I and II (see Figs. 4 and 5). Due to different elastic source moduli in Model III even for equal or similar source geometries different corresponding moment tensors, moment tensor components and magnitudes are expected. This is observed in the inversion results (see Tab. 1) and Figs. 9, 6A). Indicated by the fault-planes in Fig. 9 the retrieved source geometry indicates (small) misorientation from true source orientation. For the slip inclination we now find $\delta = 87.7°$. Thus, a larger amount of volumetric source changes is retrieved than for Model I and II. Accordingly, we find even larger non-double-couple components: DC=84.9%, CLVD=9.6%, ISO=5.5%. The strength of the retrieved source is also reduced. Coupling of source vector elements is again observed (Fig. 6B).

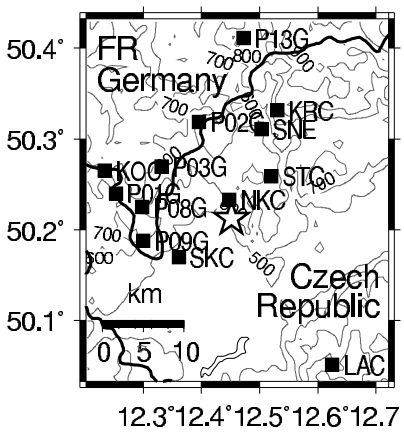

Figure 2: Distribution of stations (black squares) and seismic event (star). Hypocentre depth: 9 km. Contour lines denote altitudes above sea level. Stations PxxG were temporary stations operated by the University of Potsdam. Remaining stations are run by the Acad. Sci. of the CR.

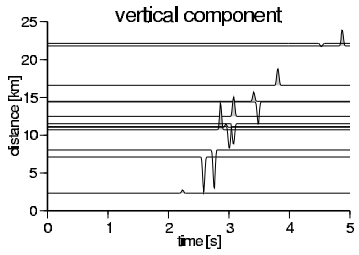

Figure 3: Vertical components of synthetic seismograms sorted according to epicentral distance for stations in 2. Anisotropy is visible by travel-time fluctuations at similar distances. Time is in seconds from source time.

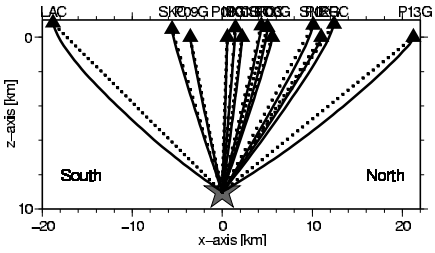

Figure 4: Vertical projection of ray paths in S-N direction from the source (star) in the models I-III to stations (triangles) given in Fig. 2. Solid lines: rays in the inhomogeneous models I and II (indistinguishable), dotted lines: rays in the homogeneous Model III. Stations from South to North: LAC, SKC, P09G, P08G, NKC, P01G, STC, KOC, P03G, SNE, P02G, KRC, P13G.

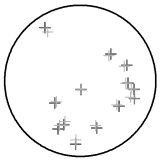

Figure 5: Take-off angles in lower hemisphere stereographic projection for rays in Model I-III and stations given in Fig. 2. Colour code (grey): dark,medium,light ⇒ Model I,II,III.

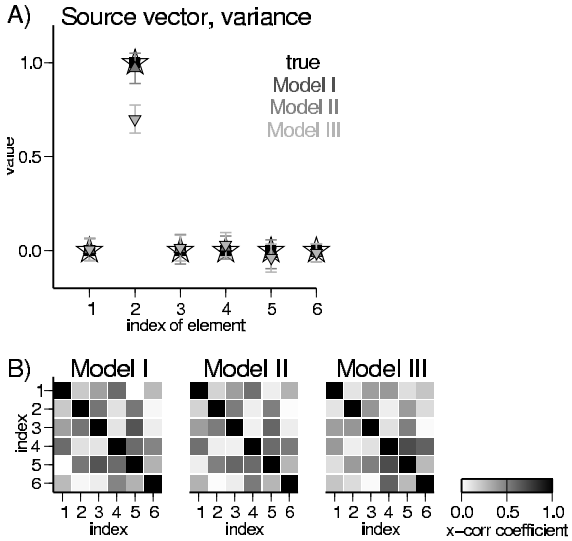

Figure 6: A: Components of the true (stars) and retrieved source vectors. For computation of the elementary seismograms Y_{ij} Model I (squares), Model II (triangles) or Model III (inverted triangles) are used. Error bars denote variances. B: Cross-correlation coefficients for the retrieved components of the source vector.

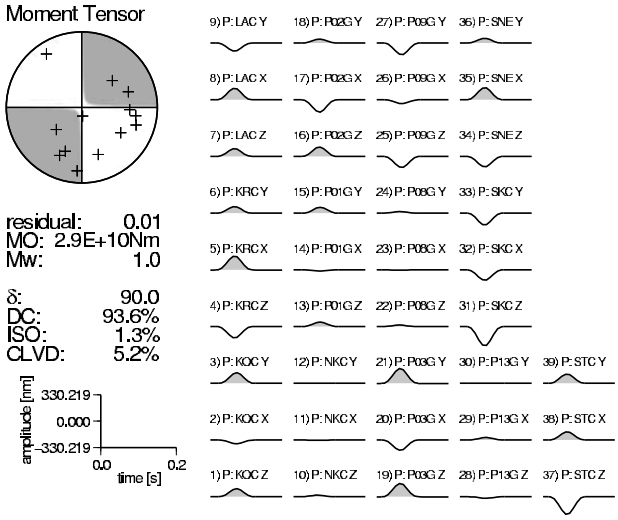

Figure 7: Characteristics of retrieved source vector in Fig. 6 using Model I and fit of waveforms.

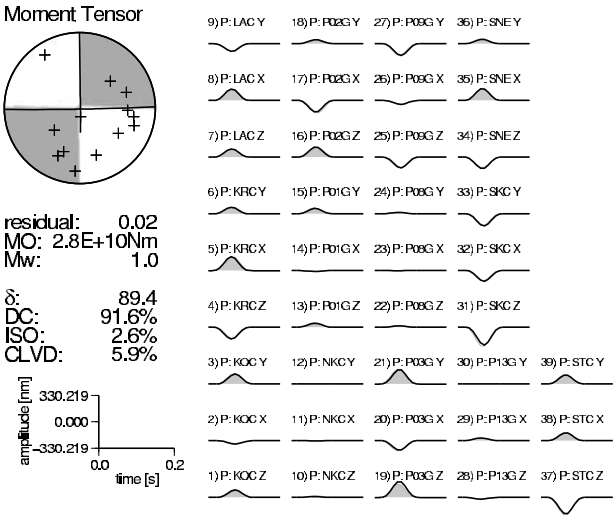

Figure 8: As in Fig. 7 but for Model II.

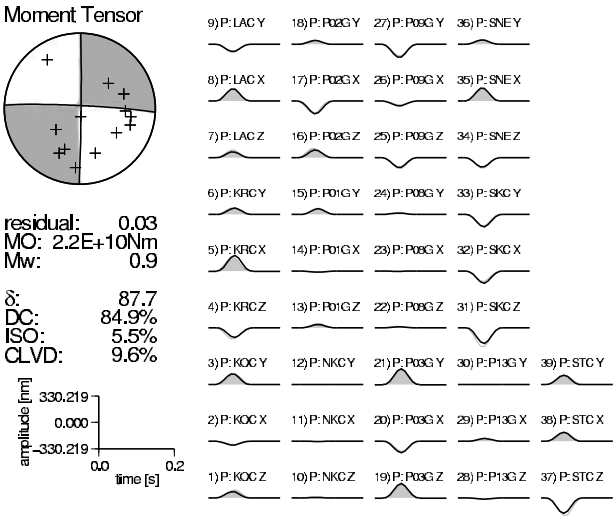

Figure 9: As in Fig. 7 but for Model III.

5 Discussion and conclusions

We have computed synthetic waveforms for direct qP-waves for one source and receivers typical for the year 2000 earthquake swarm period in W-Bohemia/Vogtland in Central Europe using a vertically inhomogeneous and anisotropic velocity model recently derived for this region. The synthetic seismograms may be differently well explained by inversion for the source vector if accurate and inaccurate velocity models are assumed. In our case these models were also derived for the same region from travel time information. They differ with respect to their degree of anisotropy and inhomogeneity. The best fitting results are obtained, of course, if the structure is correctly known. In our modelling of waveforms the velocity model is weakly anisotropic. Therefore, using the isotropic approxmation of this model (Model II) errors that occur during inversion are small and the source vector is retrieved satisfactory. Simplification of the model by a homogeneous model results in larger residuals and greater errors in source retrieval even if anisotropy is accounted for (Model III). Although we give variances of retrieved source parameters uncertainties due to structural mismodelling are difficult to quantify and must be further assessed by bootstrap tests and inversion under different model assumptions (*Šílený*, 2004).

We draw the following conclusions.

1) Inverting for the source vector instead of the moment tensor for sources in anisotropic media by accounting for anisotropy accurate yields an accurate image of the source. This allows for interpretation of the retrieved source vector in terms of volumetric source changes.

2) The success of the proposed inversion scheme depends on the accuracy of the assumed structural model. Source retrieval works well if the structural mismodelling is small.

3) Largest residual reduction occurs if (oversimplifying) homogeneous velocity models are replaced by (more correct) inhomogeneous models even if the inhomogeneous models neglect anisotropy.

4) Accounting for anisotropy in inhomogeneous models further increases the accuracy of the retrieved result.

The inversion scheme will be applied to earthquake data from the earthquake-swarm region Vogtland/W-Bohemia at the border between the Czech Republic and the FR Germany recorded during the swarm episode in 2000. Future applications can be seen in seismic regions in which accurate determination of source mechanisms is of superior interest and for which well-defined anisotropic velocity models exist, e.g. in borehole vicinity or in carbonhydrate production fields.

6 Acknowledgements

Support of the German Science Foundation (DFG, grant KR1935/1-1), of the Charles University Prague through the MAGMA project, of the Geophysical Institute, Acad. Sci. of the CR, and the consortium project SW3D is appreciated.

References

Aki, K. and Richards, P. (2002). *Quantitative Seismology*, University Science Books.

Ben-Menahem, A., Gibson Jr, R. and Sena, A. (1991). Green's tensor and radiation pattern

of point sources in general anisotropic inhomogeneous elastic media, *Geophys. J. Int.*, **107**, 297–308.

Bormann, P. (Ed.) (2002). *IASPEI New Manual of Seismological Oberservatory Practice (NMSOP)*, GeoForschungszentrum Potsdam.

Dahm, T., Horálek, J. and Šílený (2000). Comparison of absolute and relative moment tensor solutions for the January 1997 West Bohemia earthquake swarm, *Stud. Geophys. Geod.*, **44**(2), 233–250.

Farra, V. and Pšenčík, I. (2003). Properties of the zeroth-,first-, and higher-order approximations of attributes of elastic waves in weakly ansiotropic media, *J. Accout. Soc. Am.*, **114**(3), 1366–1378.

Foulger, G. R., Julian, B. R., Hill, D. P., Pitt, A. M., Malin, P. E. and Shalev, E. (2004). Non-double-couple microearthquakes at Long Valley caldera, California, provide evidence for hydraulic fracturing, *J. Volcanol. Geotherm. Res.*, **132**(1), 45–71. Doi:10.1016/S0377-0273(03)00420-7.

Gajewski, D. (1993). Radiation from a point source in general anisotropic media, *Geophys. J. Int.*, **113**, 299–317.

Horálek, J., Šílený, J., Fischer, T., Slancová, A. and Boušková, A. (2000). Scenario of the January 1997 West Bohemia earthquake swarm, *Stud. Geophys. Geod.*, **44**(4), 491–521.

Jost, M. and Herrmann, R. (1989). A student's guide to and review of moment tensors, *Seism. Res. Letters*, **60**, 37–57.

Julian, B. R., Miller, A. and Foulger, G. R. (1998). Non-double-couple earthquakes, 1. Theory, *Rev. Geophys.*, **36**(4).

Julian, B. R., Miller, A. D. and Foulger, G. R. (1997). Non-double-couple earthquake mechanisms at the Hengill-Grensdalur volcanic complex, southwest Iceland, *Geophy. Res. Lett.*, **24**(7), 743–746.

Kawasaki, I. and Tanimoto, T. (1981). Radiation patterns of body waves due to the seismic dislocation occuring in an anisotropic source medium, *Bull. Seismol. Soc. Am.*, **71**(1), 37–50.

Málek, J., Horálek, J. and Janský (2005). One-dimensional qP-wave Velocity Model of the Upper Crust for the West Bohemia/Vogtland Earthquake Swarm Region, *Stud. Geophys. Geod.*, **49**. Accepted.

Menke, W. (1989). *Geophysical Data Analysis: Discrete Inverse Theory*, Vol. 45 von *International Geophysics Series*, Harcourt Brace Jovanovich.

Pšenčík, I. and Teles, T. (1996). Point source radiation in inhomogeneous anisotropic structures, *PAGEOPH*, **148**, 591–623.

Rößler, D., Krüger, F. and Rümpker, G. (2005). Inversion for seismic moment tensors in anisotropic media using standard techniques for isotropic media, *Geophys. J. Int.*. Submitted.

Rößler, D., Rümpker, G. and Krüger, F. (2004). Ambiguous Moment Tensors and Radiation Patterns in Anisotropic Media with Applications to the Modeling of Earthquake Mechanisms in W-Bohemia, *Stud. Geophys. Geod.*, **48**(1), 233–250.

Šílený (2004). Regional moment tensor uncertainty due to mismodeling of the crust, *Tectonopysics*, **383**, 133–147.

Silver, G. P. and Jordan, T. H. (1982). Optimal estimation of the scalar seismic moment, *Geophys. J. R. astr. Soc.*, **70**, 755–787.

Solomon, S. C. and Julian, B. R. (1974). Seismic constraints on ocean-ridge mantle structure: anomalous fault plane solutions from first motions, *Geophys. J. R. astr. Soc.*, **38**, 265–285.

Sykes, L. R. (1967). Mechanism of earthquakes and nature of faulting on the mid-ocean ridges, *J. Geophys. Res.*, **72**(8), 5–27.

Vavryčuk, V. (1993). Crustal anisotropy from local observations of shear-wave splitting in West Bohemia, Czech Republic, *Bull. Seismol. Soc. Am.*, **83**(5), 1420–1441.

Vavryčuk, V. (2002). Non-double-couple earthquakes of 1997 January in West Bohemia, Czech Republic: evidence of tensile faulting, *Geophys. J. Int.*, **149**, 364–373.

Vavryčuk, V. (2005). Focal mechanisms in anisotropic media, *Geophys. J. Int.*, **161**. Doi:10.1111/j.1365-246X.2005.02585.

Wirth, W., Plenefisch, T., Klinge, K., Stammler, K. and Seidl, D. (2000). Focal mechanisms and stress field in the region Vogtland/Western Bohemia, *Stud. Geophys. Geod.*, **44**(2), 126–141.